



# Laminated graphene oxide membrane for recovery of mercury-containing wastewater by pervaporation

Ziheng Wang<sup>1</sup> · Yingzhe Qin<sup>1</sup> · Xiangping Xu<sup>2</sup> · Jiawei Sun<sup>1</sup> · Jiancheng Shen<sup>2</sup> · Xiaogang Ning<sup>2</sup> · Na Li<sup>1</sup>

Received: 1 March 2021 / Accepted: 15 June 2021 / Published online: 29 June 2021  
© The Author(s) 2021

## Abstract

Mercury (Hg) is a toxic heavy metal contaminant and has very harmful effects for human health. In this work, Hg-containing wastewater with Hg concentration of 6.36 ppb and 9.4 ppb were recovered with polyethylenimine (PEI) cross-linked graphene oxide (GO) layered membrane (c-GO-PEI) by pervaporation. The influence of ionic type, the concentration of Hg and the feed temperature were investigated. The c-GO-PEI exhibited not only high rejection for salts (> 99.97%), Hg (77.5–100%) and non-purgeable organic carbon (NPOC) (67.3–90.8%) but also high flux ( $30.30 \text{ kg}\cdot\text{m}^{-2}\cdot\text{h}^{-1}$ ) to treat with the wastewater. In addition, the flux could be largely recovered after simple washing, indicating the excellent antifouling property of the membrane.

**Keywords** Laminated graphene oxide membrane · Wastewater treatment · Mercury removal · Pervaporation

## Introduction

With the development of industrialization and urbanization, water pollution is a major concern, and the efficient treatment of wastewater is becoming a challenge. In carbonaceous fuel combustion and petrochemical industry, a large amount mercury-containing waste gas and wastewater are produced. As a toxic heavy metal, mercury (Hg) can accumulate in food chain and has long-term influence on human beings, especially the nervous system. (Yu et al. 2016) Thus, attentions should be paid to the treatment of Hg-containing wastewater. Recently, various Hg removal approaches have been developed, such as chemical precipitation, adsorption, ion exchange and membrane separation. (Azimi et al. 2017; Oehmen et al. 2014; Yu et al. 2016) However, chemical precipitation causes second pollution.

Adsorption faces the problem of ion competition. And ion exchange produces reclaimed water. Membrane separation is widely used in wastewater treatment with the advantages of low energy consumption, no chemical additives and ready coupling with other processes. (Pendergast and Hoek 2011; Samsami et al. 2020) Ultrafiltration (UF) and nanofiltration (NF) are widely employed in wastewater treatment. However, UF cannot reject small molecules and ions including  $\text{Hg}^{2+}$  because of the porous nature of UF membranes. As a pressure-driven processes, nanofiltration (NF) will face the problems of serious membrane fouling and concentration polarization when treating complex wastewater. (Kim, 2018) Moreover, the evaporation–crystallization process that has been widely used for salty water treatment is hard to attain Hg-free distillate due to the volatility of Hg. (Bin et al. 2019)

Pervaporation is a membrane-based separation method, in which the feed solution flow through the upside of the membrane and become vapor in the downside. The membrane structure could be well-tuned to make it be capable of rejecting salts (Castro-Munoz 2020; Wang et al. 2016a) and volatile components (Cao et al. 2021; Ong et al. 2016; Yang, 2019). Besides, low membrane fouling could be achieved by reducing the roughness and elevating the hydrophilicity of the membrane surface. These properties make pervaporation a promising method to treat wastewater with multiple components and obtain fresh water. Recently, wastewater treatment by pervaporation has been widely studied, aiming

✉ Jiancheng Shen  
737118508@qq.com

✉ Na Li  
lina@mail.xjtu.edu.cn

<sup>1</sup> Shaanxi Key Laboratory of Energy Chemical Process Intensification, School of Chemical Engineering and Technology, Xi'an Jiaotong University, Xi'an 710049, Shaanxi, People's Republic of China

<sup>2</sup> Shaanxi Beiyuan Chemical Group Co., Ltd, Yulin 719319, Shaanxi, People's Republic of China

to remove or recover organic compounds (Aliabadi et al. 2011, 2012; Cao et al. 2021; García et al. 2013; Kujawa et al. 2015; Li et al. 2018; Mei, 2020; Toth and Mizsey 2015; Wang et al. 2018; Wu et al. 2016; Yi and Wan 2017; Zhang et al. 2016; Zhao and Shi 2009), sulfuric acid (Cui et al. 2020; Liu et al. 2021), ammonia (Yang, 2014) and heavy metals (Baysak 2021; Nigiz 2019). Baysak (Baysak 2021) fabricated polyvinyl alcohol/NaY zeolite membranes to recover Cr from wastewater by pervaporation, and results showed that the membrane could effectively reject Cr(VI). Nigiz (Nigiz 2019) prepared poly(vinyl alcohol) membranes coated with poly(ether-block-amide) layer and investigated pervaporation desalination performance treating seawater containing lithium, copper, arsenic and lead. The composite membranes exhibited heavy metal rejections > 94%. As far as we known, the recovery of Hg by pervaporation has not yet been reported.

Recently, various materials were developed to construct pervaporation membranes, in which graphene oxide (GO) has promising prospects. GO was composed of two-dimensional hexagonal skeleton of carbon atom structure and oxygen groups, which has the properties of high strength, hydrophilicity and easy to modify. By means of filtration, coating or layer-by-layer deposition (Wei et al. 2018), GO nano flakes could be self-assembled on the substrate, forming an ultrathin dense membrane of layered structure. However, pure GO membranes are prone to swell and collapse in water condition. To strengthen the structural stability of GO membranes, a large amount of cross-linking agents were applied, including polymers (Chen et al. 2014; Cheng et al. 2017; Pan, 2020; Park et al. 2009; Suri et al. 2019; Tian et al. 2013), small molecules (An et al. 2011; Feng et al. 2016; Hung, 2014; Jia et al. 2016; Liu et al. 2020; Qian et al. 2018; Wang, 2016b; Zhang et al. 2020, 2015), ions (Chen, 2017; Gao et al. 2019; Lin and Chen 2021; Park et al. 2008; Yu et al. 2017) and nano materials (Cho, 2019; Dong et al. 2020; Shi, 2019; Xi et al. 2016). Polyethylenimine (PEI) is a kind of hydrophilic and flexible polymer, and abundant amino group endows PEI molecules with positive charge. GO was negatively charged by carboxyl group, which could react with amino group, resulting in a favorable cross-linking structure based on both electrostatic attraction and covalent bonding. The structure is hoped to improve the mechanical strength of the GO layered membrane. Besides, with PEI intercalation, the zeta potential of GO-PEI membranes could be converted to positive, and the membranes are able to reject cations (e.g.,  $\text{Hg}^{2+}$ ) by electrostatic repulsion.

Herein, PEI intercalated GO layered membrane was fabricated with pressure-assisted self-assembly method and cross-linked in acid environment. The morphology, chemical composition and hydrophilicity were investigated. The prepared membrane was applied to treat Hg-containing wastewater by pervaporation. This work enlightens a new

way to develop membranes for complex wastewater treatment, especially removal or recovery of volatile components.

## Experimental

### Materials

Graphite was purchased from Tianjin No. 1 Chemical Reagent Factory, China. Potassium permanganate ( $\text{KMnO}_4$ ), sodium nitrate ( $\text{NaNO}_3$ ), sulfuric acid ( $\text{H}_2\text{SO}_4$ ) and hydrochloric acid (HCl) were purchased from Xi Long Chemical Co., Ltd., China. Hydrogen peroxide ( $\text{H}_2\text{O}_2$ ) and sodium chloride (NaCl) were supplied by Sinopharm Chemical Reagent Co., Ltd., China. Polyethylenimine (PEI) with molecular weight of 70 000 was purchased from Shanghai Aladdin Biochemical Technology Co., Ltd. All materials and reagents were used without further treatment. Deionized (DI) water was self-made in laboratory. Mixed cellulose ester (MCE) microfiltration membranes (diameter of 80 mm and pore size of 0.22  $\mu\text{m}$ ) were purchased from Chuangwei Filter Equipment. Hg-containing wastewater was provided by Shaanxi Beiyuan Chemical Group Co., Ltd, China.

### Preparation of GO

GO was synthesized by Hummers method. First, 6 g graphite powder, 3 g  $\text{NaNO}_3$  and 138 mL  $\text{H}_2\text{SO}_4$  were mixed together under continuous stirring and 30 g  $\text{KMnO}_4$  was slowly added. The reaction was kept at 0 °C for 2 h and for another 5 h at 35 °C. Then, 276 mL DI water was progressively added into the mixture and the temperature was raised to 95 °C and kept for 30 min. After the mixture was cooled to room temperature, 840 mL DI water and 60 mL  $\text{H}_2\text{O}_2$  were added. The mixture was repeatedly washed with 3% HCl and DI water till neutral pH was achieved and then centrifuged at 8000 rpm to remove the supernatant. Finally, the sediment was dried at 50 °C in a vacuum oven and the GO was obtained.

### Preparation of c-GO-PEI membranes

Pressure-assisted self-assembly method was used to fabricate GO membranes. First, GO was dispersed in DI water by sonication to form an aqueous dispersion of 0.5 g/L. PEI was dissolved in DI water at 0.5 g/L. Then, 2 mL GO dispersion and 10 mL PEI solution were added into 200 mL DI water under stirring. The mixture was filtrated through nylon microfiltration substrate membrane and after filtration, the membrane was dried in a hot air oven at 50 °C for 4 h. Subsequently, the GO-PEI membrane was soaked in DI water at room temperature for 12 h and then in a mixture of 200 mL DI water and 2 mL HCl for reaction at 50 °C for 4 h. After

that, the membranes were dried in a hot air oven at 50 °C for 4 h. The prepared membrane was denoted as c-GO-PEI.

## Characterizations

Chemical composition of membranes was analyzed by Fourier transform infrared spectroscopy with attenuated total reflectance mode (ATR-FTIR, Thermo Fisher Scientific, Nicolet iS50) and X-ray photoelectron spectroscopy (XPS, Thermo Fisher Scientific, ESCALAB Xi+). Surface hydrophilicity was measured by water contact angle (WCA, KRÜSS, DSA100). Surface morphology was obtained with scanning electronic microscope (SEM, TESCAN, MAIA3LMH). Element distribution of membranes was analyzed by energy dispersive X-ray spectrometry (EDS, Aztec X-maxN50) on SEM. Electrokinetic analyzer (Anton Paar, SurPASS) was used to measure the zeta potential of membrane surface.

## Pervaporation performance of GO-PEI membranes

The pervaporation performance of c-GO-PEI membranes was tested with a home-made instrument, as illustrated in Fig. 1. The effective membrane area is 15.9 cm<sup>2</sup>. During the test, feed solution was heated by water bath and circulated from feed tank to the membrane surface and back to the feed tank with a peristaltic pump at flow rate of 18 L/h. The permeate was condensed with liquid nitrogen and collected with a cold trap at vacuum of 0.096 MPa. The flux ( $J$ , kg·m<sup>-2</sup>·h<sup>-1</sup>) and rejection ( $R$ , %) were calculated with following equations.

$$J = \frac{W}{A \cdot t} \quad (1)$$

where  $W$  (kg) is the weight loss of feed solution during the test,  $A$  (m<sup>2</sup>) is the effective membrane area, and  $t$  (h) is the time of the pervaporation test.

$$R = \frac{c_f - c_p}{c_f} \times 100\% \quad (2)$$

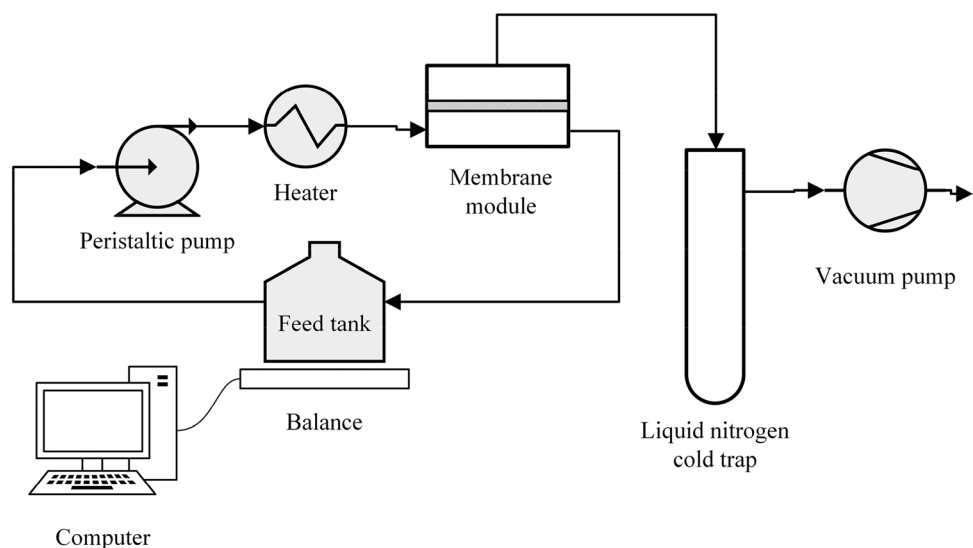
where  $c_f$  and  $c_p$  are the concentration of feed and permeate solutions, respectively.

## Characterization

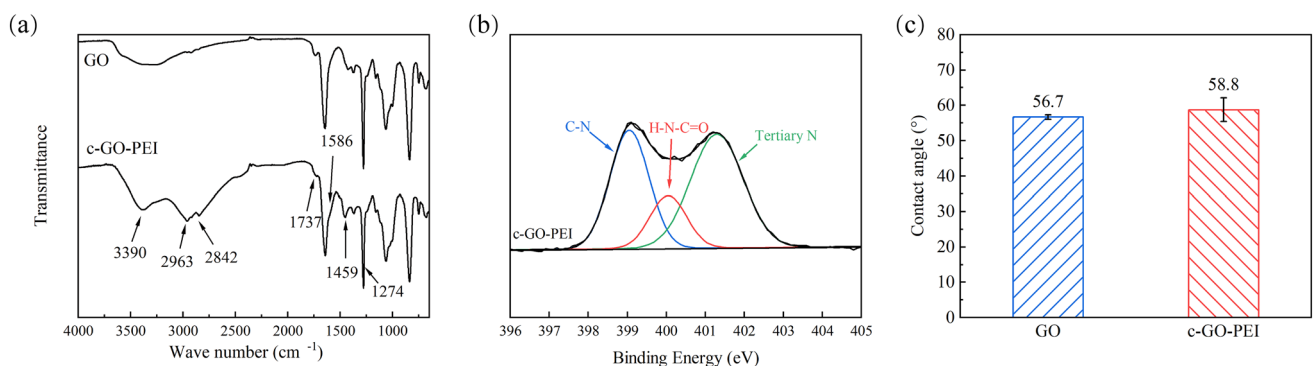
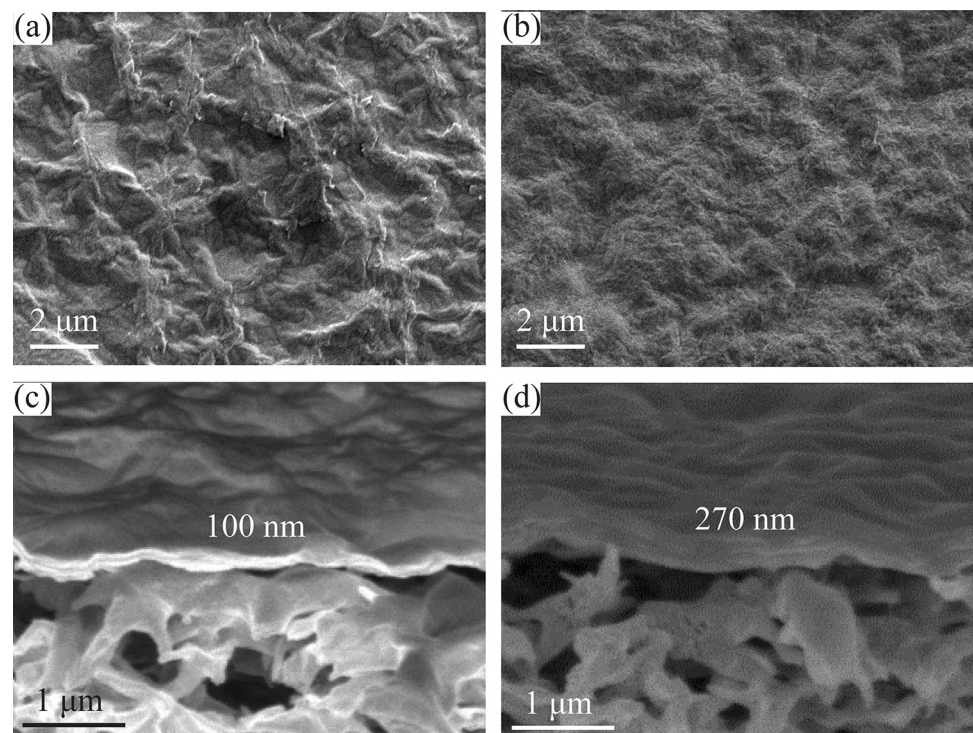
The surface images of GO and c-GO-PEI membranes were shown in Fig. 2a and b. The top layer on the MCE support is dense and demonstrates typical wrinkles of GO nanosheets. With intercalation of PEI, the wrinkles of c-GO-PEI became flatter and broader. This should be related to the interaction of the long PEI chains with GO nanosheets that could induce the spreading and flattening of GO sheets in the assembly of laminated structure. In cross-sectional view (Fig. 2c, d), it is observed that GO layers closely stacked on the substrate with a thickness of 100 nm and 270 nm for GO and c-GO-PEI membranes, respectively. The increased thickness is resultant from enlarged interlayer spacing of GO nanosheet by the intercalation of PEI. The thicker layer could also diminish the effect of coarse structure of MCE support on the morphology of the thin GO layer. The smoothed membrane surface is expected to be favorable in reducing membrane fouling.

Figure 3a shows the ATR-FTIR spectra of GO and c-GO-PEI membranes. The peaks at 3390, 1737, 1459 and 1274 cm<sup>-1</sup> represent –OH, C=O, C–O and C–O–C, respectively, indicating characteristic absorption bands of

**Fig. 1** Schematic diagram of pervaporation experiment setup



**Fig. 2** SEM images of pristine GO and c-GO-PEI membranes



**Fig. 3** **a** FTIR spectra of GO and c-GO-PEI membranes, **b** XPS N1s fitting curve of c-GO-PEI membrane and **c** water contact angles of GO and c-GO-PEI membranes

GO. For the spectrum of c-GO-PEI, characteristic peaks of N–H can be seen at  $1586\text{ cm}^{-1}$ , and C–H can be seen at  $2842$  and  $2963\text{ cm}^{-1}$ , confirming the existence of PEI and the formation of cross-linking structure in the membrane. (Guo et al. 2021; Halakoo and Feng 2020; Qian et al. 2018) In XPS N1s spectrum (Fig. 3b), the fitted peaks represent C–N at  $399.0\text{ eV}$ , N–C=O at  $400.1\text{ eV}$  and tertiary N at  $401.3\text{ eV}$ , which confirms the successful intercalation of PEI in the GO membrane. The characteristic N–C=O peak is assigned to the amide bond formed by GO and PEI in cross-linking. (Pan et al. 2020).

The water flux and antifouling performance are affected by membrane surface hydrophilicity. Figure 3c depicts the

water contact angles of GO and c-GO-PEI membranes. The pristine GO membrane exhibits a hydrophilic surface, owing to the existence of abundant oxygen-containing groups on GO. After PEI intercalation and cross-linking, the c-GO-PEI membrane still shows good hydrophilicity with water contact angle slightly increased to  $58.8^\circ$ , which is because of the consumption of oxygen groups in cross-linking. (Sun et al. 2020) In addition, it is measured that the surface zeta potential of GO membrane and c-GO-PEI membrane are  $-28.7\text{ mV}$  and  $+31.7\text{ mV}$ , respectively. The conversion of zeta potential from negative to positive value further indicates the successful hybrid of PEI in GO membrane.



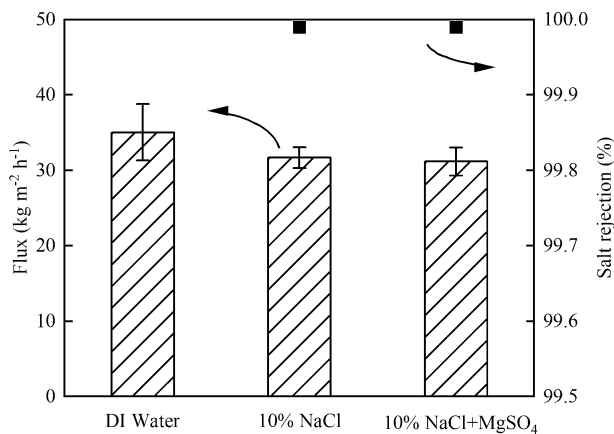


Fig. 4 PV performance of c-GO-PEI membranes

## Pervaporation performance

### Desalination test

NaCl and MgSO<sub>4</sub> were used as feed solutes to test the PV performance of membrane in treating with different salt ions. As shown in Fig. 4, the salt rejection for NaCl and mixed ion solution were both 99.99%. Besides the non-volatility of salts, the electrostatic repulsion of positively charged membrane to salt cations should also contribute to the perfect salt rejection. Due to the high salt concentration, the partial vapor pressure of feed reduced; and thus the water flux of salt solutions slightly decreased by 9.4% and 11.1% than pure water. Nevertheless, the flux of mixed ion solution is near to that of NaCl solution, indicating the good desalination performance of the membrane for complex salt solution.

### Hg-containing wastewater test

In chemical industry, Hg-containing wastewater is generally produced due to the employment of Hg-containing catalysts such as for the synthesis of polyvinyl chloride. The traditional evaporation method is limited due to the natural volatility of Hg. Pervaporation could be an effective way to remove trace Hg because of its potential of rejecting volatile components. The wastewater with two levels of Hg content, 6.36 ppb and 9.4 ppb, was used to test the PV performance of membrane for the remove of Hg and NPOC. The components of the wastewater are listed in Table 1. Hg exists in the form of HgCl<sub>2</sub> molecules and Hg ions such as Hg<sup>2+</sup>, HgCl<sup>+</sup>, HgCl<sub>3</sub><sup>-</sup> and HgCl<sub>4</sub><sup>2-</sup> (Wang et al. 2016c). The PV performance was shown in Fig. 5. It can be seen that 35vol% solution was collected in the permeate after 6 h of the concentration process, during which the flux gradually decreased because of the decline of water vapor pressure

Table 1 Contents in Hg-containing wastewater

Component	6.36 ppb Hg	9.4 ppb Hg
Hg/ppb	6.36	9.4
pH	8.17	8.21
Conductivity/mS·cm <sup>-1</sup>	107.1	102.6
NaCl/mg·L <sup>-1</sup>	7567	7248
Na <sub>2</sub> SO <sub>4</sub> /mg·L <sup>-1</sup>	1282	1228
NPOC/mg·L <sup>-1</sup>	71.74	74.56

and the inevitably increased concentration polarization while remaining a considerably high level of above 26 kg·m<sup>-2</sup>·h<sup>-1</sup> in the end (Fig. 5a). Salt rejection always maintained over 99.97% (Fig. 5b). The removal rate of Hg is higher than 90% in most cases (Fig. 5c). The membrane exhibited good rejection for NPOC component (Fig. 5d) due to the hydrophilicity of membrane which facilitates water permeation while hinders the transport of organic molecules.

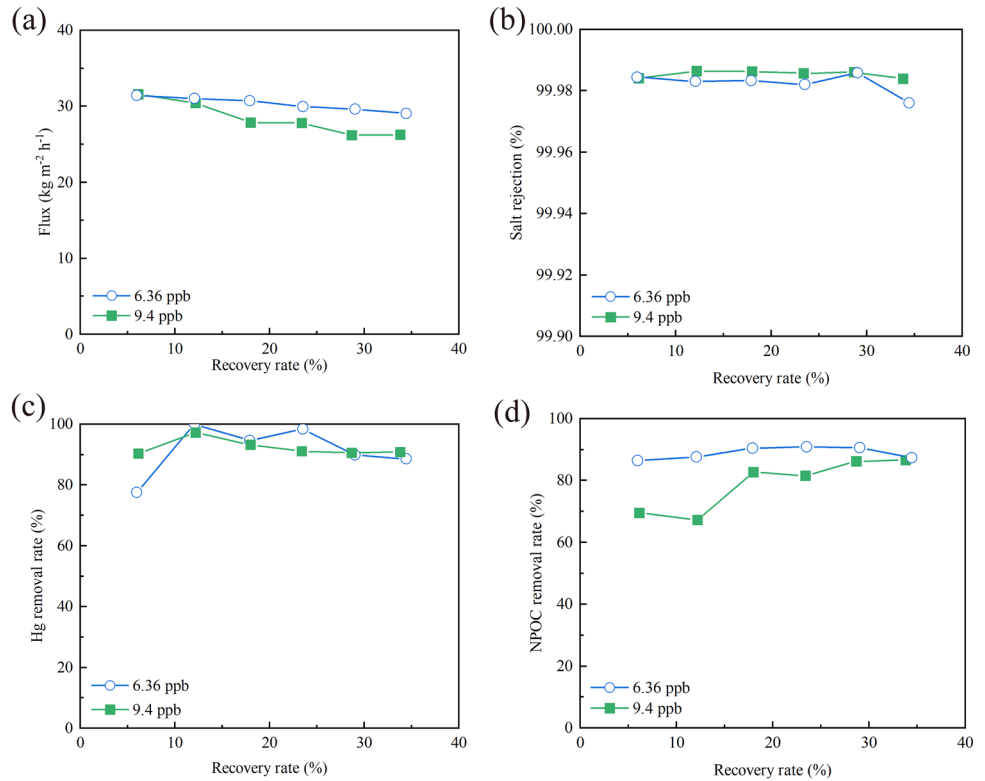
Figure 6 shows the effects of feed temperature on the flux and rejection with c-GO-PEI. The flux increases rapidly as temperature increases from 55 to 75 °C, which is because of the rise of water vapor pressure and intensified motion of PEI chains with temperature. The flux with wastewater containing 6.36 ppb Hg was lower than that containing 9.4 ppb Hg, which is related to the higher salt concentration of the former solution. At the same time, the rejections to salt, Hg and NPOC remained at high levels, which means c-GO-PEI could perform well at a wide range of temperature. Figure 7 shows that, by the one-step PV process, the clear permeate was obtained from the yellow wastewater samples. All the results indicate the good efficiency of the PV process with c-GO-PEI membrane in the wastewater treatment.

### Antifouling test

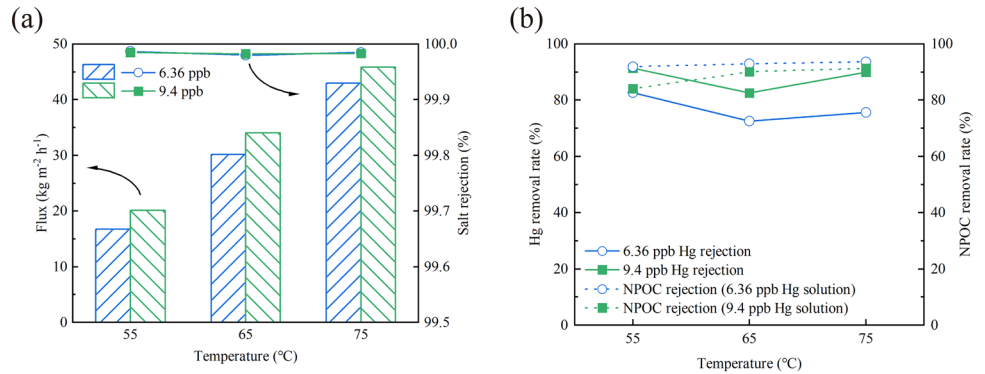
To study the fouling and Hg adsorption of the membranes, after the PV experiment (Fig. 6), the morphology and element distribution of membrane surface was analyzed by SEM and EDS. By EDS analysis, it is found that Hg mass fraction on membrane are 2.53% and 2.84% for c-GO-PEI membranes tested with 6.36 ppb and 9.4 ppb wastewater, respectively, which are lower than 3.84% for the pristine GO membrane. This should be related to the repulsion capability of positively charged PEI-modified membrane to Hg in the wastewater. The SEM images (Fig. 8) show less pollutant that adsorbed on the top surface of c-GO-PEI membranes compared to that on the pristine membrane, which confirms the improved antifouling property of the PEI-modified membrane.

Moreover, Hg adsorption content was estimated by mass balance calculation and illustrated in Table. 2. The

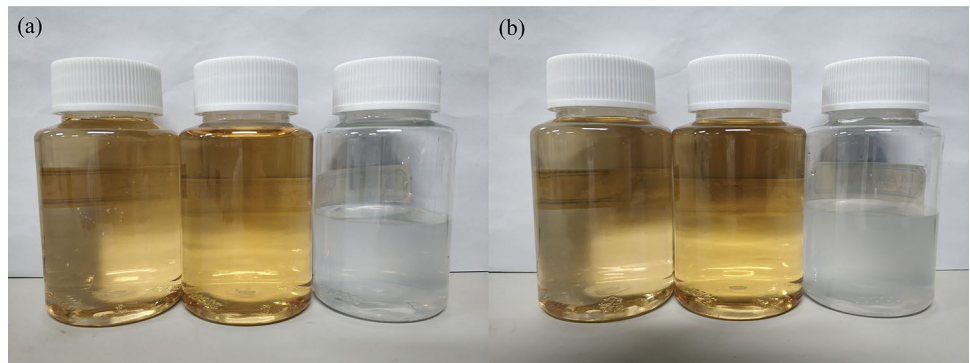
**Fig. 5** Pervaporation performance of c-GO-PEI: **a** Flux, **b** Salt rejection, **c** Hg rejection, **d** NPOC removal rate (Operating temperature: 65 °C)



**Fig. 6** Pervaporation performance of c-GO-PEI at different temperatures: **a** Flux and salt rejection; **b** Hg and NPOC removal rates



**Fig. 7** Photographs of Hg-containing wastewater samples before and after PV treatment. **a** 6.36 ppb feed solution, PV retentate solution and PV permeate; **b** 9.4 ppb feed solution, PV retentate solution and PV permeate (from left to right)



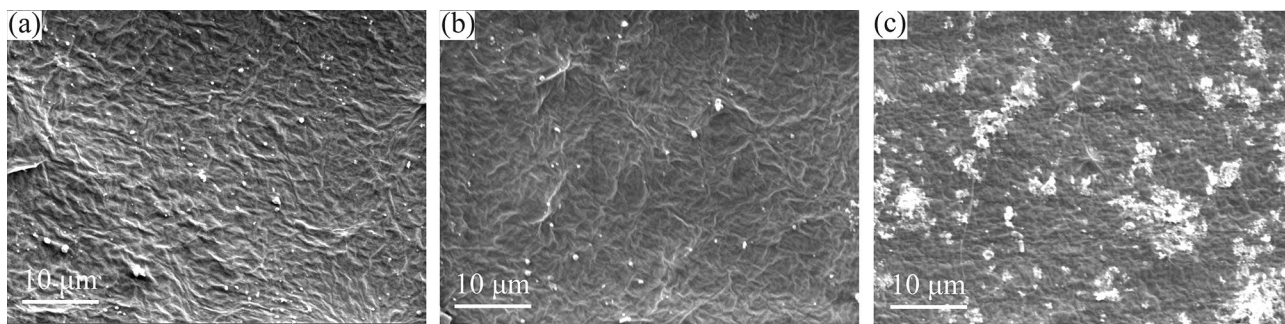
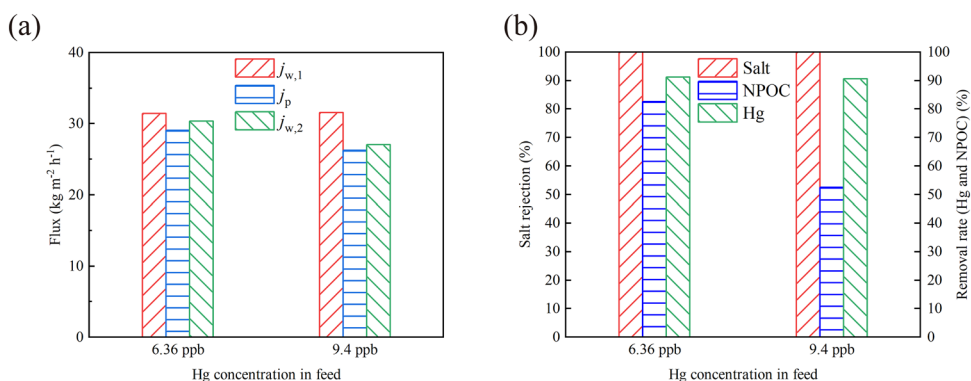


**Fig. 8** Surface morphology of membranes after PV test. **a** c-GO-PEI (6.36 ppb Hg wastewater); **b** c-GO-PEI (9.4 ppb Hg wastewater); **c** pristine GO membrane (9.4 ppb Hg wastewater)

**Table. 2** Mass balance calculation of Hg-containing wastewater test

Hg concentration in feed /ppb	Mass of feed /g	Hg concentration in concentrated feed /ppb	Mass of concentrated feed /g	Hg concentration in permeate /ppb	Mass of permeate /g	Hg content ratio
6.36	850.9	10.46	547.7	0.54	303.2	1.09
9.4	832.2	15.84	539.2	0.73	293	1.12

**Fig. 9** Antifouling performance of c-GO-PEI membrane in treating with Hg-containing wastewaters. (a) Flux; (b) Salt rejection and removal rates of NPOC and Hg (Operating temperature: 65 °C)



Hg content ratios are very closed to one, indicating the Hg adsorption is slight on the membrane during the PV test.

$$\text{Hg content ratio} = \frac{\text{Hg content in concentrated feed} + \text{Hg content in permeate}}{\text{Hg content in feed}} \quad (3)$$

The antifouling property of membrane was further investigated in terms of flux recovery ratio and fouling ratio. After the PV concentration test with Hg-containing wastewater for 6 h (Fig. 5), the membranes were rinsed with 500 mL DI water for 10 min, which was repeated for three times. After washing, the PV performance of membrane were tested for one hour at 65 °C, after which four parameters are calculated by Eqs. 4-7: FRR (flux recovery ratio),  $R_t$  (total fouling ratio),  $R_r$  (reversible fouling ratio) and  $R_{ir}$  (irreversible fouling ratio), where  $j_{w,1}$  and  $j_p$  are the fluxes of the first and the last hour in PV concentrating test, and  $j_{w,2}$  is the flux of the cleaned membrane.

**Table 3** Antifouling parameters of c-GO-PEI treating Hg-containing wastewater

Hg concentration in feed	FRR (%)	$R_t$ (%)	$R_r$ (%)	$R_{ir}$ (%)
6.36 ppb	96.69	7.45	4.14	3.31
9.4 ppb	85.72	16.81	2.53	14.28

As shown in Fig. 9a, the fluxes were largely recovered after the simply washing, and the retention to the solutes remained high (Fig. 9b). The results of FRR,  $R_r$  and  $R_{ir}$  are listed in Table. 3, which indicate good antifouling property of the membrane. The membrane remained an intact and clear surface after the long-term usage and washing (Fig. 10). The results indicate the reliability of membrane in treating with the wastewater.



**Fig. 10** Digital photographs of c-GO-PEI membranes before (left) and after test with 6.36 ppb (center) and 9.4 ppb (right) Hg-containing wastewaters that washed with DI water

$$FRR = \frac{j_{w,2}}{j_{w,1}} \times 100\% \quad (4)$$

$$R_t = \frac{j_{w,1} - j_p}{j_{w,1}} \times 100\% \quad (5)$$

$$R_r = \frac{j_{w,2} - j_p}{j_{w,1}} \times 100\% \quad (6)$$

$$R_{ir} = \frac{j_{w,1} - j_{w,2}}{j_{w,1}} \times 100\% = R_t - R_r \quad (7)$$

## Conclusion

In this study, c-GO-PEI membrane was prepared to recover Hg-containing wastewater by pervaporation. The membrane shows high flux and almost all salts and Hg were rejected by c-GO-PEI attributed to the electrostatic repulsion between ions and the membrane surface. Due to the positively charged, hydrophilic and smooth membrane surface, the flux could be well recovered by simple washing. This work provides a new approach for treating wastewater with salts, heavy metals and organic components.

**Acknowledgements** We would thank Prof. Youlong Xu and his students at Xi'an Jiaotong University for their kind help with the measurement of surface zeta potential of membrane.

**Funding** This work was supported by the National Natural Science Foundation of China (Grant Number 21676210) and the Enterprise Joint Foundation of Shaanxi Science and Technology Department in China (Grant Number 2019JLM-23).

## Declarations

**Conflict of interest** The authors declare no conflicts of interest to this work.

**Ethical approval** All the authors have made significant contributions to this work. Informed consent was obtained from all individual participant included in the study.

**Open Access** This article is licensed under a Creative Commons Attribution 4.0 International License, which permits use, sharing, adaptation, distribution and reproduction in any medium or format, as long as you give appropriate credit to the original author(s) and the source, provide a link to the Creative Commons licence, and indicate if changes were made. The images or other third party material in this article are included in the article's Creative Commons licence, unless indicated otherwise in a credit line to the material. If material is not included in the article's Creative Commons licence and your intended use is not permitted by statutory regulation or exceeds the permitted use, you will need to obtain permission directly from the copyright holder. To view a copy of this licence, visit <http://creativecommons.org/licenses/by/4.0/>.

## References

- Aliabadi M, Aroujalian A, Raisi A (2011) Pervaporative removal of acrylonitrile from aqueous streams through polydimethylsiloxane membrane. *Water Sci Technol* 63:2820–2826. <https://doi.org/10.2166/wst.2011.612>
- Aliabadi M, Aroujalian A, Raisi A (2012) Removal of styrene from petrochemical wastewater using pervaporation process. *Desalination* 284:116–121. <https://doi.org/10.1016/j.desal.2011.08.044>
- An Z, Compton OC, Putz KW, Brinson LC, Nguyen ST (2011) Bio-inspired borate cross-linking in ultra-stiff graphene oxide thin films. *Adv Mater* 23:3842–3846. <https://doi.org/10.1002/adma.201101544>
- Azimi A, Azari A, Rezakazemi M, Ansarpour M (2017) Removal of heavy metals from industrial wastewaters: a review. *Chembioeng Rev* 4:37–59. <https://doi.org/10.1002/cben.201600010>
- Baysak FK (2021) A novel approach to Chromium rejection from sewage wastewater by pervaporation. *J Mol Struct* 1233:130082. <https://doi.org/10.1016/j.molstruc.2021.130082>
- Bin H, Yang Y, Cai L, Yang L, Roszak S (2019) Enhancing mercury removal across air pollution control devices for coal-fired power plants by desulfurization wastewater evaporation. *Environ Technol* 40:154–162. <https://doi.org/10.1080/09593330.2017.1380716>
- Cao XT, Wang KA, Feng XS (2021) Removal of phenolic contaminants from water by pervaporation. *J Membr Sci* 623:119043. <https://doi.org/10.1016/j.memsci.2020.119043>
- Castro-Munoz R (2020) Breakthroughs on tailoring pervaporation membranes for water desalination: a review. *Water Res* 187:116428. <https://doi.org/10.1016/j.watres.2020.116428>
- Chen L et al (2017) Ion sieving in graphene oxide membranes via cationic control of interlayer spacing. *Nature* 550:380–383. <https://doi.org/10.1038/nature24044>
- Chen L, Huang L, Zhu J (2014) Stitching graphene oxide sheets into a membrane at a liquid/liquid interface. *Chem Commun (Camb)* 50:15944–15947. <https://doi.org/10.1039/c4cc07558g>
- Cheng C, Shen LD, Yu XF, Yang Y, Wang XF (2017) Robust construction of a graphene oxide barrier layer on a nanofibrous substrate assisted by the flexible poly(vinylalcohol) for efficient pervaporation desalination. *J Mater Chem A* 5:3558–3568. <https://doi.org/10.1039/c6ta09443k>



- Cho KM et al (2019) Ultrafast-selective nanofiltration of an hybrid membrane comprising laminated reduced graphene oxide/graphene oxide nanoribbons. *ACS Appl Mater Interfaces* 11:27004–27010. <https://doi.org/10.1021/acsami.9b09037>
- Cui KJ, Li P, Zhang R, Cao B (2020) Preparation of pervaporation membranes by interfacial polymerization for acid wastewater purification. *Chem Eng Res Des* 156:171–179. <https://doi.org/10.1016/j.cherd.2020.01.022>
- Dong LL, Li MH, Zhang S, Si XJ, Bai YX, Zhang CF (2020) NH<sub>2</sub>-Fe<sub>3</sub>O<sub>4</sub>-regulated graphene oxide membranes with well-defined laminar nanochannels for desalination of dye solutions. *Desalination* 476:114227. <https://doi.org/10.1016/j.desal.2019.114227>
- Feng B, Xu K, Huang AS (2016) Covalent synthesis of three-dimensional graphene oxide framework (GOF) membrane for seawater desalination. *Desalination* 394:123–130. <https://doi.org/10.1016/j.desal.2016.04.030>
- Gao Y, Su KM, Wang XT, Li ZH (2019) A metal-nano GO frameworks/PPS membrane with super water flux and high dyes interception. *J Membr Sci* 574:55–64. <https://doi.org/10.1016/j.memsci.2018.12.052>
- García V, Pongrácz E, Phillips PS, Keiski RL (2013) From waste treatment to resource efficiency in the chemical industry: recovery of organic solvents from waters containing electrolytes by pervaporation. *J Clean Prod* 39:146–153. <https://doi.org/10.1016/j.jclepro.2012.08.020>
- Guo J, Bao HF, Zhang YQ, Shen X, Kim JK, Ma J, Shao L (2021) Unravelling intercalation-regulated nanoconfinement for durably ultrafast sieving graphene oxide membranes. *J Membr Sci*. <https://doi.org/10.1016/j.memsci.2020.118791>
- Halakoo E, Feng XS (2020) Layer-by-layer assembly of polyethyleneimine/graphene oxide membranes for desalination of high-salinity water via pervaporation. *Sep Purif Technol* 234:116077. <https://doi.org/10.1016/j.seppur.2019.116077>
- Hung WS et al (2014) Cross-linking with diamine monomers to prepare composite graphene oxide-framework membranes with varying d-spacing. *Chem Mater* 26:2983–2990. <https://doi.org/10.1021/cm5007873>
- Jia ZQ, Wang Y, Shi WX, Wang JL (2016) Diamines cross-linked graphene oxide free-standing membranes for ion dialysis separation. *J Membr Sci* 520:139–144. <https://doi.org/10.1016/j.memsci.2016.07.042>
- Kim S et al (2018) Removal of contaminants of emerging concern by membranes in water and wastewater: a review. *Chem Eng J* 335:896–914. <https://doi.org/10.1016/j.cej.2017.11.044>
- Kujawa J, Cerneaux S, Kujawski W (2015) Highly hydrophobic ceramic membranes applied to the removal of volatile organic compounds in pervaporation. *Chem Eng J* 260:43–54. <https://doi.org/10.1016/j.cej.2014.08.092>
- Li D, Yao J, Sun H, Liu B, Li DY, van Agtmaal S, Feng CH (2018) Preparation and characterization of SiO<sub>2</sub>/PDMS/PVDF composite membrane for phenols recovery from coal gasification wastewater in pervaporation. *Chem Eng Res Des* 132:424–435. <https://doi.org/10.1016/j.cherd.2018.01.045>
- Lin CH, Chen WH (2021) Influence of water, H<sub>2</sub>O<sub>2</sub>, H<sub>2</sub>SO<sub>4</sub>, and NaOH filtration on the surface characteristics of a graphene oxide-iron (GO-Fe) membrane. *Sep Purif Technol* 262:118317. <https://doi.org/10.1016/j.seppur.2021.118317>
- Liu SY, Hu KW, Cerruti M, Barthelat F (2020) Ultra-stiff graphene oxide paper prepared by directed-flow vacuum filtration. *Carbon* 158:426–434. <https://doi.org/10.1016/j.carbon.2019.11.007>
- Liu HQ, Xia JZ, Cui KJ, Meng JQ, Zhang R, Cao B, Li P (2021) Fabrication of high-performance pervaporation membrane for sulfuric acid recovery via interfacial polymerization. *J Membr Sci* 624:119108. <https://doi.org/10.1016/j.memsci.2021.119108>
- Mei X et al (2020) A novel system for zero-discharge treatment of high-salinity acetonitrile-containing wastewater: combination of pervaporation with a membrane-aerated bioreactor. *Chem Eng J* 384:123338. <https://doi.org/10.1016/j.cej.2019.123338>
- Nigiz FU (2019) Preparation and performance of ultra-thin surface coated pervaporation membranes for seawater purification. *Water Supply* 19:1778–1784. <https://doi.org/10.2166/ws.2019.053>
- Oehmen A, Vergel D, Fradinho J, Reis MA, Crespo JG, Velizarov S (2014) Mercury removal from water streams through the ion exchange membrane bioreactor concept. *J Hazard Mater* 264:65–70. <https://doi.org/10.1016/j.jhazmat.2013.10.067>
- Ong YK, Shi GM, Le NL, Tang YP, Zuo J, Nunes SP, Chung TS (2016) Recent membrane development for pervaporation processes. *Prog Polym Sci* 57:1–31. <https://doi.org/10.1016/j.progpolymsci.2016.02.003>
- Pan FS et al (2020) Graphene oxide membranes with fixed interlayer distance via dual crosslinkers for efficient liquid molecular separations. *J Membr Sci* 595:117486. <https://doi.org/10.1016/j.memsci.2019.117486>
- Park S, Dikin DA, Nguyen ST, Ruoff RS (2009) Graphene oxide sheets chemically cross-linked by polyallylamine. *J Phys Chem C* 113:15801–15804. <https://doi.org/10.1021/jp907613s>
- Park S, Lee KS, Bozoklu G, Cai W, Nguyen ST, Ruoff RS (2008) Graphene oxide papers modified by divalent ions-enhancing mechanical properties via chemical cross-linking. *ACS Nano* 2:572–578. <https://doi.org/10.1021/nm700349a>
- Pendergast MM, Hoek EMV (2011) A review of water treatment membrane nanotechnologies. *Energy Environ Sci* 4:1946–1971. <https://doi.org/10.1039/c0ee00541j>
- Qian YL, Zhou C, Huang AS (2018) Cross-linking modification with diamine monomers to enhance desalination performance of graphene oxide membranes. *Carbon* 136:28–37. <https://doi.org/10.1016/j.carbon.2018.04.062>
- Samsami S, Mohamadi M, Sarrafzadeh MH, Rene ER, Firoozbahr M (2020) Recent advances in the treatment of dye-containing wastewater from textile industries: overview and perspectives. *Process Saf Environ Prot* 143:138–163. <https://doi.org/10.1016/j.psep.2020.05.034>
- Shi B et al (2019) Control of edge/in-plane interactions toward robust, highly proton conductive graphene oxide membranes. *ACS Nano* 13:10366–10375. <https://doi.org/10.1021/acs.nano.9b04156>
- Sun JW, Qian XW, Wang ZH, Zeng FX, Bai HC, Li N (2020) Tailoring the microstructure of poly(vinyl alcohol)-intercalated graphene oxide membranes for enhanced desalination performance of high-salinity water by pervaporation. *J Membr Sci* 599:117838. <https://doi.org/10.1016/j.memsci.2020.117838>
- Suri A, Calzavarini L, Strunck AB, Magnacca G, Boffa V (2019) Comparison of chemical cross-linkers with branched and linear molecular structures for stabilization of graphene oxide membranes and their performance in ethanol dehydration. *Ind Eng Chem Res* 58:18788–18797. <https://doi.org/10.1021/acs.iecr.9b01532>
- Tian Y, Cao Y, Wang Y, Yang W, Feng J (2013) Realizing ultrahigh modulus and high strength of macroscopic graphene oxide papers through crosslinking of mussel-inspired polymers. *Adv Mater* 25:2980–2983. <https://doi.org/10.1002/adma.201300118>
- Toth AJ, Mizsey P (2015) Methanol removal from aqueous mixture with organophilic pervaporation: experiments and modelling. *Chem Eng Res Des* 98:123–135. <https://doi.org/10.1016/j.cherd.2015.04.031>
- Wang SF et al (2016b) A highly permeable graphene oxide membrane with fast and selective transport nanochannels for efficient carbon capture. *Energy Environ Sci* 9:3107–3112. <https://doi.org/10.1039/c6ee01984f>

- Wang QZ, Li N, Bolto B, Hoang M, Xie ZL (2016a) Desalination by pervaporation: a review. *Desalination* 387:46–60. <https://doi.org/10.1016/j.desal.2016.02.036>
- Wang Y, Mei X, Ma TF, Xue CJ, Wu MD, Ji M, Li YG (2018) Green recovery of hazardous acetonitrile from high-salt chemical wastewater by pervaporation. *J Clean Prod* 197:742–749. <https://doi.org/10.1016/j.jclepro.2018.06.239>
- Wang YJ, Tian Y, Zang WC, Jian XD (2016c) Study on treatment and recycling of mercury from waste mercury catalysts in China. *Procedia Environ Sci* 31:432–439. <https://doi.org/10.1016/j.proenv.2016.02.090>
- Wei Y, Zhang YS, Gao XL, Ma Z, Wang XJ, Gao CJ (2018) Multilayered graphene oxide membranes for water treatment: a review. *Carbon* 139:964–981. <https://doi.org/10.1016/j.carbon.2018.07.040>
- Wu XM, Zhang QG, Soyekwo F, Liu QL, Zhu AM (2016) Pervaporation removal of volatile organic compounds from aqueous solutions using the highly permeable PIM-1 membrane. *AIChE J* 62:842–851. <https://doi.org/10.1002/aic.15077>
- Xi YH, Hu JQ, Liu Z, Xie R, Ju XJ, Wang W, Chu LY (2016) Graphene oxide membranes with strong stability in aqueous solutions and controllable lamellar spacing. *ACS Appl Mater Interfaces* 8:15557–15566. <https://doi.org/10.1021/acsami.6b00928>
- Yang X et al (2014) A pervaporation study of ammonia solutions using molecular sieve silica membranes. *Membranes (basel)* 4:40–54. <https://doi.org/10.3390/membranes4010040>
- Yang G et al (2019) Functionalizing graphene oxide framework membranes with sulfonic acid groups for superior aqueous mixture separation. *J Mater Chem A* 7:19682–19690. <https://doi.org/10.1039/c9ta04031e>
- Yi SL, Wan YH (2017) Volatile organic compounds (VOCs) recovery from aqueous solutions via pervaporation with vinyltriethoxysilane-grafted-silicalite-1/polydimethylsiloxane mixed matrix membrane. *Chem Eng J* 313:1639–1646. <https://doi.org/10.1016/j.cej.2016.11.061>
- Yu WZ, Yu TY, Graham N (2017) Development of a stable cation modified graphene oxide membrane for water treatment. *2d Materials* 4:045006. <https://doi.org/10.1088/2053-1583/aa814c>
- Yu JG, Yue BY, Wu XW, Liu Q, Jiao FP, Jiang XY, Chen XQ (2016) Removal of mercury by adsorption: a review. *Environ Sci Pollut Res Int* 23:5056–5076. <https://doi.org/10.1007/s11356-015-5880-x>
- Zhang YL, Benes NE, Lammertink RGH (2016) Performance study of pervaporation in a microfluidic system for the removal of acetone from water. *Chem Eng J* 284:1342–1347. <https://doi.org/10.1016/j.cej.2015.09.084>
- Zhang M, Mao Y, Liu G, Liu G, Fan Y, Jin W (2020) Molecular bridges stabilize graphene oxide membranes in water. *Angew Chem Int Ed Engl* 59:1689–1695. <https://doi.org/10.1002/anie.201913010>
- Zhang Y, Zhang S, Chung TS (2015) Nanometric graphene oxide framework membranes with enhanced heavy metal removal via nanofiltration. *Environ Sci Technol* 49:10235–10242. <https://doi.org/10.1021/acs.est.5b02086>
- Zhao W, Shi BL (2009) Removal of volatile organic compounds from water by pervaporation using polyetherimide-polyethersulfone blend hollow fiber membranes. *Sep Sci Technol* 44:1737–1752. <https://doi.org/10.1080/01496390902775851>

**Publisher's Note** Springer Nature remains neutral with regard to jurisdictional claims in published maps and institutional affiliations.